nature medicine

5′-triphosphate-siRNA: turning gene silencing and Rig-I activation against melanoma

Hendrik Poeck[1–3,12], Robert Besch[4,12], Cornelius Maihoefer[2,3,12], Marcel Renn[5,12], Damia Tormo[5], Svetlana Shulga Morskaya[6], Susanne Kirschnek[7], Evelyn Gaffal[5], Jennifer Landsberg[5], Johannes Hellmuth[1], Andreas Schmidt[2], David Anz[2], Michael Bscheider[2,3], Tobias Schwerd[2], Carola Berking[4], Carole Bourquin[2], Ulrich Kalinke[8], Elisabeth Kremmer[9], Hiroki Kato[10], Shizuo Akira[10], Rachel Meyers[6], Georg Häcker[7], Michael Neuenhahn[7], Dirk Busch[7], Jürgen Ruland[3], Simon Rothenfusser[2], Marco Prinz[11], Veit Hornung[1], Stefan Endres[2], Thomas Tüting[5] & Gunther Hartmann[1]

Genetic and epigenetic plasticity allows tumors to evade single-targeted treatments. Here we direct *Bcl2*-specific short interfering RNA (siRNA) with 5′-triphosphate ends (3p-siRNA) against melanoma. Recognition of 5′-triphosphate by the cytosolic antiviral helicase retinoic acid–induced protein I (Rig-I, encoded by *Ddx58*) activated innate immune cells such as dendritic cells and directly induced expression of interferons (IFNs) and apoptosis in tumor cells. These Rig-I–mediated activities synergized with siRNA-mediated *Bcl2* silencing to provoke massive apoptosis of tumor cells in lung metastases *in vivo*. The therapeutic activity required natural killer cells and IFN, as well as silencing of *Bcl2*, as evidenced by rescue with a mutated *Bcl2* target, by site-specific cleavage of *Bcl2* messenger RNA in lung metastases and downregulation of Bcl-2 protein in tumor cells *in vivo*. Together, 3p-siRNA represents a single molecule–based approach in which Rig-I activation on both the immune- and tumor cell level corrects immune ignorance and in which gene silencing corrects key molecular events that govern tumor cell survival.

Cellular transformation and progressive tumor growth result from an accumulation of genetic and epigenetic changes that alter normal cell proliferation and survival pathways[1]. Tumor pathogenesis is accompanied by a process called cancer immunoediting, a temporal transition from immune-mediated tumor elimination in early phases of tumor development to immune escape of established tumors. IFNs have emerged as central coordinators of these tumor–immune system interactions[2]. Owing to their plasticity, tumors tend to evade single-targeted therapeutic approaches designed to control proliferation and survival of tumor cells[3] and even evade immunotherapies that are directed at multiple tumor antigens[4]. There are good reasons to believe that a combinatorial approach that suppresses tumor cell survival and at the same time increases immunogenicity of tumor cells could lead to more effective tumor treatments[5,6].

Short double-stranded RNA (dsRNA) oligonucleotides are excellent candidates for such a combinatorial approach[7]. These short dsRNA molecules can be designed to target mRNA encoding key regulators of tumor survival through the mechanism of RNA interference (RNAi)[8,9]. A distinct and independent biological property of RNA oligonucleotides is their ability to activate immunoreceptors specialized for the detection of viral nucleic acids. The ubiquitously expressed helicase Rig-I is one of two immunoreceptors that signal the presence of viral RNA in the cytosol of cells[10]. Specifically, Rig-I detects RNA with a triphosphate group at the 5′ end[11,12]. Formation of such 5′-triphosphate RNA by RNA polymerases in the cytosol of cells is characteristic for most negative-stranded RNA viruses[13].

Because recognition of 5′-triphosphate RNA by Rig-I is largely independent of the RNA sequence and gene silencing is not inhibited by the presence of a 5′-triphosphate, both biological activities can be elicited by one short dsRNA molecule (3p-siRNA). Such 3p-siRNAs were described to induce type I IFN[14]. 3p-siRNA can be designed to target the mRNA of any key tumor survival factor. In the case of melanoma, such a molecule is Bcl-2, which was originally found in B cell lymphomas and is involved in the regulation of apoptosis.

[1]Institute of Clinical Chemistry and Pharmacology, University Hospital, University of Bonn, Sigmund-Freud-Strasse 25, 53127 Bonn, Germany. [2]Division of Clinical Pharmacology, Department of Internal Medicine, Ludwig-Maximilians University, Ziemssenstrasse 1, 80336 Munich, Germany. [3]III. Medizinische Klinik, Klinikum rechts der Isar, Technische Universität München, Ismaninger Strasse 15, 81675 Munich, Germany. [4]Department of Dermatology and Allergology, Ludwig-Maximilians-University, Thalkirchner Strasse 48, 80337 Munich, Germany. [5]Laboratory for Experimental Dermatology, Department of Dermatology and Allergology, University of Bonn, Sigmund-Freud-Strasse 25, 53105 Bonn, Germany. [6]Alnylam Pharmaceuticals, 300 Third Street, Cambridge, Massachusetts 02142, USA. [7]Institute for Medical Microbiology, Immunology and Hygiene, Technische Universität München, Trogerstrasse 30, 81675 Munich, Germany. [8]Division of Immunology, Paul-Ehrlich-Institut, Paul-Ehrlich-Strasse 51-59, 63225 Langen, Germany. [9]Institute of Molecular Immunology, Helmholtz Zentrum München, Marchioninistrasse 25, 81377 Munich, Germany. [10]Department of Host Defense, Research Institute for Microbial Diseases, Osaka University, Osaka 565-0871, Japan. [11]Department of Neuropathology, University of Freiburg, Breisacherstrasse 64, 79106 Freiburg, Germany. [12]These authors contributed equally to this work. Correspondence should be addressed to T.T. (thomas.tueting@ukb.uni-bonn.de) or G. Hartmann (gunther.hartmann@ukb.uni-bonn.de).

Received 20 August; accepted 3 October; published online 2 November 2008; doi:10.1038/nm.1887

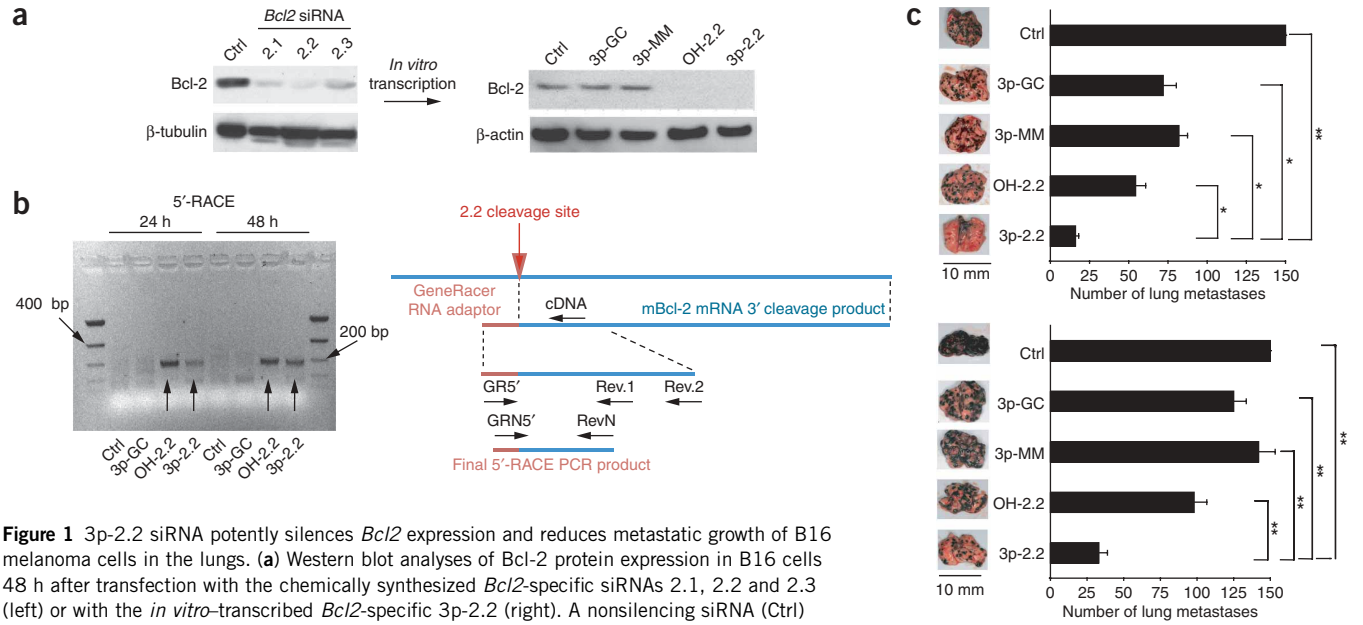

Figure 1 3p-2.2 siRNA potently silences *Bcl2* expression and reduces metastatic growth of B16 melanoma cells in the lungs. (**a**) Western blot analyses of Bcl-2 protein expression in B16 cells 48 h after transfection with the chemically synthesized *Bcl2*-specific siRNAs 2.1, 2.2 and 2.3 (left) or with the *in vitro*–transcribed *Bcl2*-specific 3p-2.2 (right). A nonsilencing siRNA (Ctrl) served as negative control at left, whereas the 5′-triphosphate RNAs 3p-GC and mismatch 3p-MM served as negative controls at right. One representative experiment of four is shown. (**b**) Left, *in vitro* 5′-RACE analysis of RNA extracted from B16 cells 24 h after treatment with the indicated RNAs. Black vertical arrows mark the 5′-RACE PCR amplification product showing the predicted product of RNAi (334 base pair (bp) expected size). Right, schematic diagram showing the position of the predicted *Bcl2* cleavage site relative to nested primers used for PCR amplification of the cleavage fragment. (**c**) Images showing lung metastases after intravenous challenge of C57BL/6 mice with B16 melanoma cells and treatment with 50 μg of the indicated RNAs intravenously on days 3, 6 and 9 after 12 d (top) or 17 d (bottom). The mean numbers of macroscopically visible melanoma metastases for each group (± s.e.m.) are depicted to the right of the images. $*P < 0.05$ or $**P < 0.01$; Mann-Whitney *U* test.

Overexpression of *Bcl2* is considered to be responsible for the extraordinary resistance of melanoma cells to chemotherapy[15–17]. Here we developed 3p-siRNA that simultanously silences *Bcl2* and activates RIG-I and study the use of this bifunctional RNA molecule for tumor therapy.

RESULTS

Antitumor efficacy of *Bcl2*-specific 3p-siRNA

We tested three synthetic siRNAs targeting different regions of mouse *Bcl2* mRNA for their ability to downregulate Bcl-2 protein in B16 melanoma cells (**Fig. 1a** and **Supplementary Table 1** online). The activity and the specificity of *Bcl2* downregulation was maintained when *Bcl2*-specific siRNA contained a 5′-triphosphate (**Fig. 1a** and **Supplementary Table 2** online). 3p-2.2, the most effective *Bcl2*-specific 3p-siRNA, and OH-2.2, the synthetic siRNA counterpart without 5′-triphosphate groups, were selected for further experiments. The 3p-RNA oligonucleotides 3p-GC (a GC-rich sequence) and 3p-MM (a sequence similar to 3p-2.2 but with mismatches at bases 9–11) were used as controls. Silencing of Bcl-2 by 3p-2.2 was specific, as expression of the prosurvival Bcl-2 family members Mcl-1 and Bcl-xL and of the proapoptotic BH3-only Bcl-2 family members Puma and Bim was not inhibited (**Supplementary Fig. 1** online). Using rapid amplification of cDNA ends (RACE) technology and sequencing, we could show that *Bcl2* silencing generated specific cleavage products, confirming RNAi (**Fig. 1b**).

Next we examined the antitumor activity of 3p-2.2 in the B16 melanoma lung metastasis model *in vivo*. We treated mice with RNA molecules on days 3, 6 and 9 after tumor cell inoculation and assessed growth of lung metastases on day 12 or day 17. OH-2.2 (which has gene silencing activity but is not expected to have Rig-I ligand activity) and the 3p-RNA oligonucleotides 3p-MM and 3p-GC (which have Rig-I ligand activity but are not expected to have gene silencing activity) inhibited the growth of melanoma metastases to a certain degree (**Fig. 1c**). However, 3p-2.2, which combines *Bcl2*-specific gene silencing and immunostimulatory properties, conferred significantly ($*P < 0.05$) enhanced therapeutic antitumor activity (**Fig. 1c**).

Because 5′-triphosphate RNA is known to stimulate type I IFN by activating Rig-I, we sought to evaluate the contribution of type I IFN to the antitumor effect. Experiments in type I IFN receptor–knockout mice (*Ifnar1*$^{-/-}$) confirmed that the observed antitumor activity of 3p-2.2 *in vivo* depends on intact type I IFN signaling (**Fig. 2a**). It has been reported that siRNA can be detected by Toll-like receptor 7 (TLR7) in a sequence-dependent manner, leading to type I IFN production[18,19]. We found that the number of metastases was strongly reduced upon treatment with 3p-2.2 in *Tlr7*-deficient mice, suggesting that TLR7 is not required for the antitumor activity of 3p-2.2 (**Fig. 2a**). This indicates that Rig-I, not TLR7, mediates 3p-2.2 recognition and that type I IFN induction has a dominant role in the antitumor activity. Depletion studies showed that the antitumor activity of 3p-2.2 in the B16 melanoma model depends on natural killer (NK) cells but not CD8$^+$ T cells (**Fig. 2b**).

Innate immune responses and induction of apoptosis

Next, we studied stimulation of specific immune cell subsets *in vitro*. In plasmacytoid dendritic cells, TLR7 activation is sufficient to induce the production of IFN-α. In contrast, conventional dendritic cells (cDCs) produce IFN-α in response to viral infection[20] but not to TLR7 activation. 3p-MM, 3p-GC and 3p-2.2 induced similar amounts of IFN-α in cDCs, whereas OH-2.2 was inactive (**Fig. 3a**). 3p-RNA did not induce IFN-α in B cells, NK cells or T cells (**Supplementary Fig. 2a** online). Studies with dendritic cells isolated from mice genetically deficient in either *Tlr7* or the cytosolic helicases *Ifih1* (encoding melanoma differentiation-associated protein-5 (Mda5)) or *Ddx58* (encoding Rig-I) confirmed that the induction of IFN-α

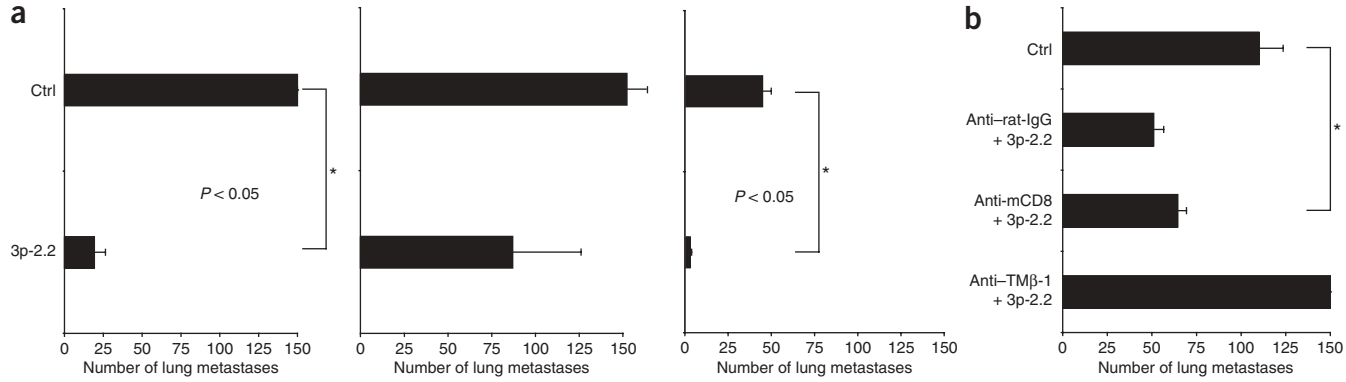

Figure 2 Activation of type I IFNs and NK cells are necessary for the antitumor activity of *Bcl2*-specific 3p-siRNA *in vivo*. (**a**) Mean numbers of macroscopically visible melanoma metastases (± s.e.m.) after intravenous challenge of wild-type (WT, left), *Ifnar1*-deficient (*Ifnar1*$^{-/-}$; middle) or *Tlr7*$^{-/-}$ (right) C57BL/6 mice with B16 melanoma cells and treatment with 50 μg of the indicated RNAs intravenously on days 3, 6 and 9. $^*P < 0.05$ ($n = 4$). (**b**) Effect of antibody-based depletion of CD8 T cells (Anti-mCD8), NK cells (Anti–TM-1) or control antibody (Anti–rat-IgG) on the therapeutic antitumor efficacy of 3p-2.2 in C57BL/6 WT mice. $^*P < 0.05$ ($n = 5$).

in cDCs by 3p-2.2 and 3p-GC depends on Rig-I but not Mda5 or TLR7 (**Supplementary Fig. 2**). No induction of apoptosis was observed in cDCs or other lymphocyte subsets exposed to 3p-2.2 (**Fig. 3b**).

Because Rig-I is broadly expressed in many cell types[21,22], we examined direct induction of type I IFN in B16 melanoma cells. 3p-2.2, 3p-MM or 3p-GC stimulated similar levels of *Ifnb1* promoter reporter gene activity in B16 cells, OH-2.2 or phosphatase-treated 3p-2.2 induced no response (**Fig. 3c**). Resting B16 melanoma cells expressed little Rig-I; however, Rig-I expression was strongly upregulated in the presence of exogenous IFN-β or 3p-2.2 (**Fig. 3d**). B16 cells treated with 3p-2.2 or 3p-GC but not OH-2.2 secreted the chemokine inducible protein-10 (IP-10) and upregulated major histocompatibility complex (MHC) class I (**Supplementary Fig. 3a,b** online). Type I IFN induction in B16 tumor cells was Rig-I dependent, as inhibition of Rig-I expression by *Ddx58*-specific siRNA or overexpression of

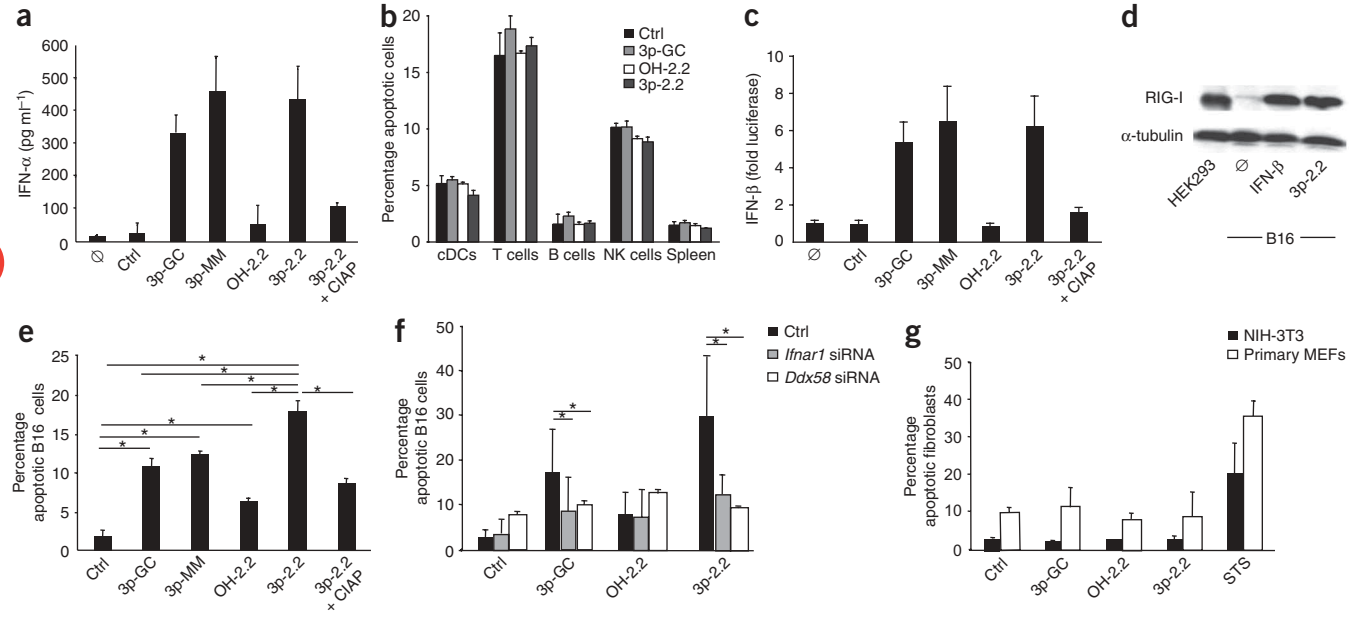

Figure 3 Bcl-2-specific 3p-siRNA induces cell type specific innate immune responses and apoptosis *in vitro*. (**a**) IFN-α concentration in the culture supernatant of cDCs, as measured by ELISA 24 h after transfection with the indicated RNAs. Data are shown as means ± s.e.m. of two independent experiments. Ø, medium; ctrl, control siRNA (**Supplementary Table 1**). (**b**) Flow cytometric analysis of apoptosis induction in cultured cDCs and freshly isolated B cells, T cells, NK cells and whole spleen cells 48 h after transfection with the indicated RNAs. Results are shown as means ± s.e.m. of two independent experiments. (**c**) Analysis of *Ifnb1* promoter activation in B16 cells 24 h after transfection with the indicated RNAs. Results of luciferase measurements are shown as means ± s.e.m. (**d**) Western blot analysis of Rig-I expression in B16 cells 8 h after treatment with 3p-2.2 (1 μg ml^{-1}) or mouse IFN-β (1,000 U ml^{-1}). HEK293 cells overexpressing Rig-I served as positive control. (**e**) Flow cytometric analysis of apoptosis induction in B16 cells 48 h after transfection with the indicated RNAs. Results are shown as mean ± s.e.m. of four independent experiments ($^*P < 0.05$; *t*-test). (**f**) Flow cytometric analysis of apoptosis induction in B16 cells 48 h after cotransfection with the indicated RNAs in combination with siRNA to *Ifnar1* or *Ddx58*. Data are shown as means ± s.e.m. of three independent experiments ($^*P < 0.05$; *t*-test). (**g**) Flow cytometric analysis of apoptosis induction in primary mouse embryonal fibroblasts (MEFs) and immortalized mouse fibroblasts (NIH-3T3) treated as indicated. Exposure to staurosporine (STS) served as a positive control.

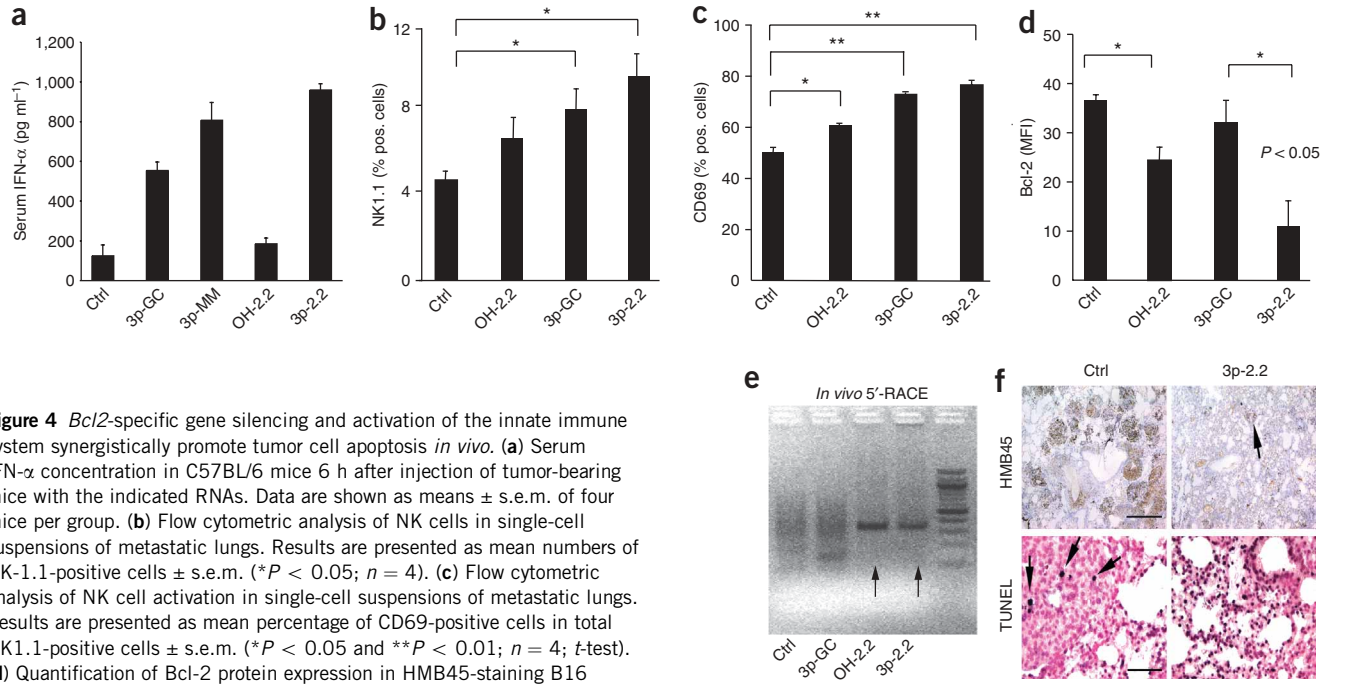

Figure 4 *Bcl2*-specific gene silencing and activation of the innate immune system synergistically promote tumor cell apoptosis *in vivo*. (**a**) Serum IFN-α concentration in C57BL/6 mice 6 h after injection of tumor-bearing mice with the indicated RNAs. Data are shown as means ± s.e.m. of four mice per group. (**b**) Flow cytometric analysis of NK cells in single-cell suspensions of metastatic lungs. Results are presented as mean numbers of NK-1.1-positive cells ± s.e.m. (*$P < 0.05$; $n = 4$). (**c**) Flow cytometric analysis of NK cell activation in single-cell suspensions of metastatic lungs. Results are presented as mean percentage of CD69-positive cells in total NK1.1-positive cells ± s.e.m. (*$P < 0.05$ and **$P < 0.01$; $n = 4$; *t*-test). (**d**) Quantification of Bcl-2 protein expression in HMB45-staining B16 tumor cells derived from single-cell suspensions of metastatic lungs. Depicted is the mean fluorescence intensity (MFI) ± s.e.m. (*$P < 0.05$ between; $n = 4$; *t*-test). (**e**) *In vivo* 5′-RACE analysis of RNA extracted from metastatic lungs. (**f**) Immunohistochemical visualization of melanoma cells (black arrow) in lung tissue sections of tumor-bearing mice (top) and detection of apoptotic cells (black arrows) within metastases by TUNEL staining (bottom). Representative sections of one experiment with five mice per group are shown. Scale bars, 300 μm (top) and 50 μm (bottom).

NS3-4A (a serine protease encoded by hepatitis C virus *HCVgp1* that cleaves interferon-β promoter stimulator 1 (refs. 23,24), a key signaling molecule of Rig-I also known as Cardif, MAVS or VISA) both eliminated the type I IFN response (**Supplementary Fig. 3c,d**). These data indicate that 3p-RNA is able to activate type I IFN directly through Rig-I in tumor cells.

3p-2.2 siRNA was designed to promote the induction of apoptosis via silencing of the antiapoptotic protein Bcl-2. Indeed, 3p-2.2 strongly induced apoptosis in B16 melanoma cells (**Fig. 3e**). Apoptosis induction with 3p-2.2 was substantially higher than with OH-2.2 alone, suggesting that Rig-I contributes to the apoptosis induction mediated by 3p-2.2 (**Fig. 3e,f**). Furthermore, apoptosis induction by 3p-GC and 3p-2.2 was reduced in the absence of *Ifnar1* (**Fig. 3f** and **Supplementary Fig. 3e**), suggesting that type I IFN signaling is involved in sensitizing tumor cells to Rig-I. Unlike B16 tumor cells, fibroblasts were not sensitive toward apoptosis induction mediated by silencing of *Bcl2* (OH-2.2), activation of Rig-I (3p-GC) or the combination of both (3p-2.2; **Fig. 3g**). Together with the lack of apoptosis induction in immune cell subsets (**Fig. 3b**), these results indicate that downregulation of Bcl-2 and activation of Rig-I preferentially lead to apoptosis of melanoma cells and suggest a relative tumor selectivity of this approach.

Next, we studied 3p-2.2–induced innate immune responses in C57BL/6 mice *in vivo*. 3p-2.2 treatment induced high systemic levels of IFN-α, interleukin-12 p40 subunit (IL-12p40) and Ifn-γ (**Fig. 4a** and **Supplementary Fig. 4** online). IFN-α was largely derived from $CD11c^+$ dendritic cells, as evidenced by the removal of this cell type in CD11c-DTR mice, as described in detail in **Supplementary Figure 4**. T helper type 1 cytokine induction by 3p-2.2 *in vivo* was dominated by Rig-I, with minor contribution from TLR7 (**Supplementary Fig. 4**). Cytokine production was dose dependent and transient (**Supplementary Fig. 5a–c** online). Treated mice showed reduced counts of lymphocytes and thrombocytes but not erythrocytes, presumably owing to systemic IFN, but there were no other obvious toxicities (**Supplementary Fig. 5d–f**). *Ex vivo* analysis of spleen cells from the treated mice showed potent activation of myeloid and plasmacytoid dendritic cells, NK cells, CD4 and CD8 T cells (**Supplementary Fig. 6** online). Activation of splenic NK cells was observed in wild-type and TLR7-deficient mice and required the presence of the type I IFN receptor; NK cells showed *ex vivo* tumoricidal activity against B16 melanoma cells (**Supplementary Fig. 7** online). Treatment with 3p-2.2 was associated with enhanced recruitment and activation of NK cells in the lungs (**Fig. 4b,c**).

Contribution of gene silencing

Confocal microscopy confirmed that fluorescently labeled siRNA reached healthy lung tissue as well as metastases (**Supplementary Fig. 8a**). *Bcl2* was silenced in tumor cells (**Fig. 4d**) of tumor-bearing mice treated with 3p-2.2 and OH-2.2 (**Fig. 4d** and **Supplementary Fig. 8b**). Downregulation of *Bcl2* was associated with RNAi *in vivo*, because only the *Bcl2*-specific siRNAs generated the expected cleavage product, as determined by 5′-RACE (**Fig. 4e**). Tunel staining revealed massive apoptosis in tumor cells of mice treated with 3p-2.2 compared with mice treated with control RNA. The number of tumor cells stained by HMB45, a mouse monoclonal antibody that recognizes melanoma cells, was much higher in the control-treated mice (**Fig. 4f**). No *Bcl2* silencing or induction of apoptosis was seen in immune cell subsets of 3p-2.2–treated mice *in vivo* (**Supplementary Fig. 8c**), further supporting the relative tumor cell selectivity of 3p-2.2.

Next, we performed rescue experiments to confirm that silencing of *Bcl2* contributes to the therapeutic activity of *Bcl2*-specific 3p-siRNA *in vivo*. B16 melanoma cells were stably transduced with a mutated

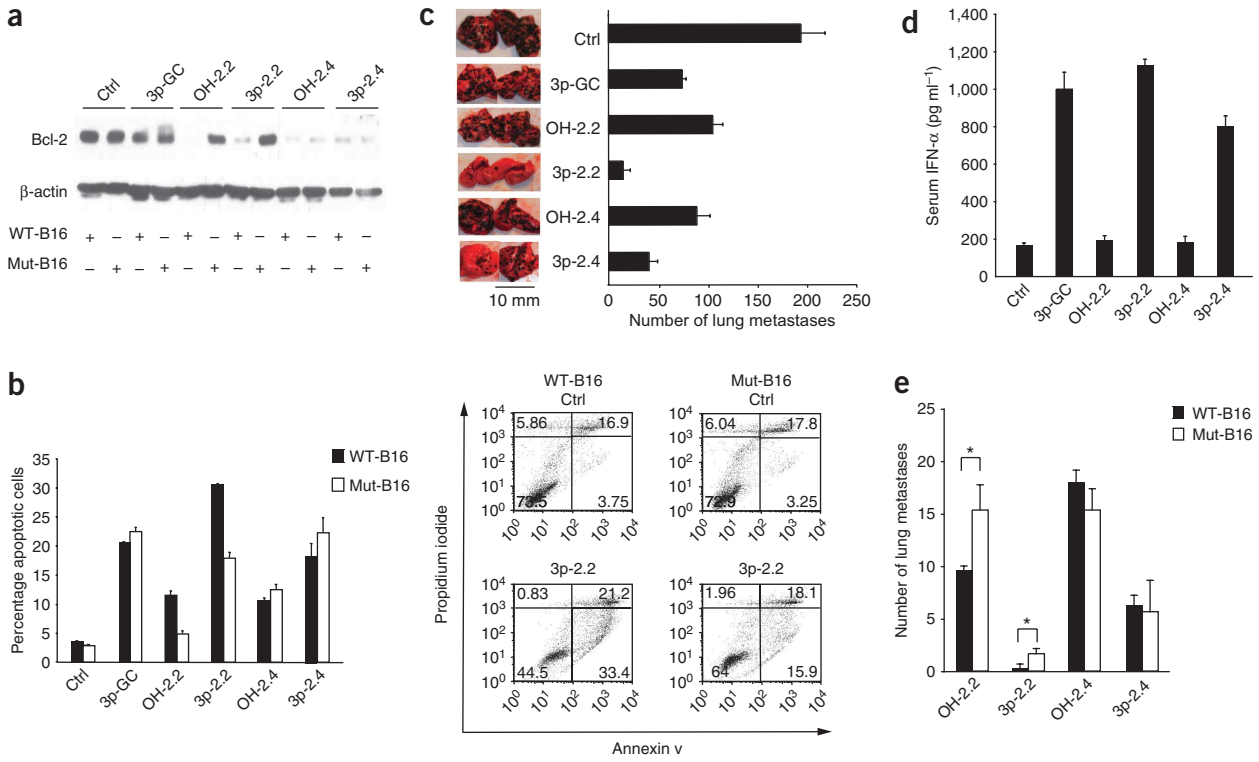

Figure 5 *Bcl2*-specific gene silencing contributes to *Bcl2*-specific 3p-siRNA–induced inhibition of tumor growth and apoptosis. (**a**) Western blot analysis of Bcl-2 protein expression in B16 cells stably transfected with WT *Bcl2* (WT-B16) or a specifically mutated *Bcl2* cDNA (Mut-B16) after treatment with the indicated RNAs. (**b**) Flow cytometric analysis of apoptosis induction in WT-B16 or Mut-B16 cells 48 h after transfection with the indicated RNAs. Results are shown as mean percentage of apoptotic cells ± s.e.m. of three independent experiments. One representative dot plot of three independent experiments is shown on the right. (**c**) Images show lung metastases after intravenous challenge of C57BL/6 mice with B16 melanoma cells and treatment with the indicated RNAs. The mean numbers of macroscopically visible melanoma metastases for each group (± s.e.m.) are depicted on the right. (**d**) Serum IFN-α concentration 6 h after treatment of tumor-bearing mice with the indicated RNAs. Data are shown as means ± s.e.m. of four mice per group. (**e**) Mean number (± s.e.m.) of macroscopically visible melanoma metastases on the lung surface after intravenous challenge of C57BL/6 mice with WT-B16 or Mut-B16 melanoma cells and treatment with the indicated RNAs. $*P < 0.01$, Mann-Whitney *U* test.

Bcl2 complementary DNA specifically designed to disrupt the target cleavage site of the *Bcl2*-specific siRNA 2.2 without affecting the amino acid sequence of the Bcl-2 protein (**Supplementary Fig. 9** online). Expression of the mutated *Bcl2* cDNA in B16 melanoma cells (Mut-B16 cells) prevented *Bcl2* silencing and apoptosis induction by 3p-2.2 but not by 3p-2.4, which targets *Bcl2* mRNA at a different, non-mutated site (**Fig. 5a**,**b** and **Supplementary Table 1**).

In vivo, 3p-2.4 and 3p-2.2 showed similar antitumor efficacy against B16 melanoma lung metastases (**Fig. 5c**) and induced similar systemic levels of IFN-α (**Fig. 5d**). Rescue experiments with wild-type B16 and Mut-B16 cells confirmed that the therapeutic effect of OH-2.2 and 3p-2.2 depends in part on *Bcl2* gene silencing in tumor cells (**Fig. 5e**). Taken together, these results provide evidence that both gene silencing and Rig-I–dependent activation of innate immunity contribute to the antitumor activity of 3p-2.2 in the B16 melanoma model *in vivo*.

Efficacy in other tumor models and in the human system

Next we confirmed the antitumor activity of 3p-siRNA in a new genetic melanoma model that imitates the molecular pathogenesis of human melanoma[25]. Primary melanomas derived from the skin of mice overexpressing hepatocyte growth factor and carrying a germline mutation in the *Cdk4* gene (Hgf–*Cdk4*^{R24C} mice) were serially transplanted to groups of *Cdk4*^{R24C} mice. Repetitive peritumoral injections with 3p-2.2 led to a significant delay in tumor growth (**Fig. 6a**) that was associated with downregulation of Bcl-2 but not Mcl-1, Bcl-xL, Puma or Bim in melanoma cells *in vivo* (**Fig. 6a**). In addition, 3p-2.2 also showed significant antitumor efficacy in a colon carcinoma model in BALB/c mice (**Fig. 6b**) that was associated with systemic production of IFN-α and downregulation of Bcl-2 expression (**Fig. 6b** and **Supplementary Fig. 10** online).

Finally, we designed human *BCL2*-specific siRNAs (OH-h2.2 and 3p-h2.2) and tested them in a human melanoma cell line (1205 Lu). Treatment of 1205Lu cells with 3p-h2.2 and 3p-GC, but not with OH-h2.2 or the control RNA, was able to induce IFN-β (**Fig. 6c**). Both OH-h2.2 and 3p-h2.2 strongly reduced BCL-2 protein abundance (**Fig. 6d**). Similarly to 3p-2.2 in mouse B16 melanoma cells, 3p-h2.2 strongly promoted apoptosis (**Fig. 6d**) and decreased viability of human melanoma cells, whereas the proapoptotic activity was less pronounced in primary human melanocytes and primary human fibroblasts, both isolated from skin of healthy donors (**Fig. 6e**).

DISCUSSION

The results of this study demonstrate that systemic administration of an siRNA deliberately designed to silence *Bcl2* and activate Rig-I (3p-2.2) strongly inhibits tumor growth, reflected by massive tumor apoptosis on a histological level. This response requires type I IFN and NK cells and is associated with the induction of systemic T helper type 1 cytokines (IFN-α, IL-12p40 and IFN-γ), direct and indirect

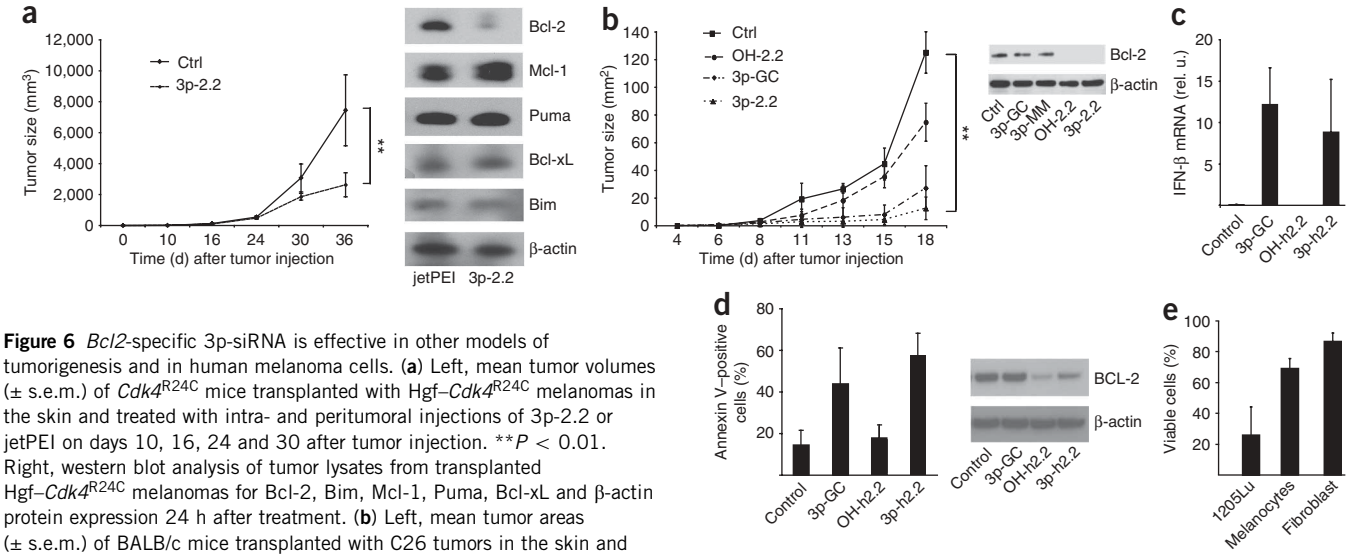

Figure 6 *Bcl2*-specific 3p-siRNA is effective in other models of tumorigenesis and in human melanoma cells. (**a**) Left, mean tumor volumes (± s.e.m.) of *Cdk4*^{R24C} mice transplanted with Hgf–*Cdk4*^{R24C} melanomas in the skin and treated with intra- and peritumoral injections of 3p-2.2 or jetPEI on days 10, 16, 24 and 30 after tumor injection. $^{**}P < 0.01$. Right, western blot analysis of tumor lysates from transplanted Hgf–*Cdk4*^{R24C} melanomas for Bcl-2, Bim, Mcl-1, Puma, Bcl-xL and β-actin protein expression 24 h after treatment. (**b**) Left, mean tumor areas (± s.e.m.) of BALB/c mice transplanted with C26 tumors in the skin and treated with intravenous injections of the indicated RNAs on days 6, after tumor injection. $^{**}P < 0.01$. Right, western blot analysis of Bcl-2 protein expression 48 h after transfection of C26 cells with the indicated RNAs. (**c**) Quantitative RT-PCR analysis of the activation of IFN-β RNA expression after treatment of 1205Lu cells with the indicated siRNAs. The mean ± s.d. of three independent experiments is shown. (**d**). Left, flow cytometric analysis of apoptosis induction in 1205Lu cells treated with the RNAs as described in **c**. The means ± s.d. of three independent experiments are shown. Right, assessment of *BCL2*-silencing activity by immunoblotting. Representative results of three independent experiments are depicted. (**e**) Viability of 1205Lu cells (three independent experiments, means ± s.d.), of human primary melanocytes and human primary fibroblasts (both isolated from three different donors) 24 h after transfection with 3p-h2.2.

activation of immune cell subsets and recruitment and activation of NK cells in lung tissue. Furthermore, sequence-specific silencing of *Bcl2* contributes to the antitumor efficacy of 3p-2.2. This is evidenced by site-specific cleavage of *Bcl2* mRNA, sequence-dependent rescue *in vitro* and *in vivo* and downregulation of Bcl-2 protein on a single-cell level in lung tumor cells.

Owing to its molecular design, siRNA 3p-2.2 contains two distinct functional properties: gene silencing and Rig-I activation. A number of biological effects caused by these two properties may cooperate to provoke the beneficial antitumor response *in vivo*. Silencing of *Bcl-2* may induce apoptosis in cells that depend on Bcl-2 overexpression (such as tumor cells) and, via the same mechanism, may also sensitize tumor cells toward innate effector cells[26]. Likewise, because Rig-I is expressed in immune cells as well as in nonimmune cells including tumor cells, activation of Rig-I leads to direct and indirect activation of immune cell subsets. It also provokes innate responses directly in tumor cells, such as the production of type I IFN or chemokines, and directly promotes apoptosis. These activities act in concert to elicit the observed potent antitumor effect.

In fact, our data provide experimental evidence that B16 melanoma cells express Rig-I and that 3p-2.2 not only silences *Bcl2* but also stimulates type I IFN, IP-10 and MHC class I and induces apoptosis directly in tumor cells. Furthermore, we show that silencing of *Bcl2* in tumor cells does not require Rig-I ligand activity (as indicated by experiments with OH-2.2, which has the same sequence as 3p-2.2 but no triphosphate) and that Rig-I effects are independent of *Bcl2* silencing activity (as indicated by experiments with 3p-MM and 3p-GC, which have the triphosphate but no silencing sequence). Notably, compared to the respective single activities, our data show synergistic induction of tumor cell apoptosis *in vitro* and synergistic inhibition of *Bcl2* and induction of apoptosis in tumor cells *in vivo* when both silencing and Rig-I activity are in place (as indicated by experiments with 3p-2.2 compared to OH-2.2, 3p-MM or 3p-GC alone).

The lower antitumor response induced by 3p-MM and 3p-GC compared to 3p-2.2 *in vivo*, the lack of *Bcl2* inhibition in tumor cells *in vivo* induced by the Rig-I ligand (3p-GC) alone, and the sequence-specific rescue experiments confirm that gene silencing is a key functional property of 3p-2.2. Likewise, the lower overall antitumor response induced by *Bcl2*-specific siRNA (OH-2.2), despite its strong inhibition of *Bcl2* in tumor cells *in vivo*, highlights the importance of the innate immune contribution. Each mechanism by itself is not as potent in suppressing tumor growth *in vivo* as is the combination of the two. This is supported by the rescue experiments, which showed that apoptosis induced by OH-2.2 depended completely on *Bcl2*, whereas apoptosis induced by 3p-2.2 depended only in part on *Bcl2* gene silencing.

A key question is how systemic administration of the bifunctional RNA molecule 3p-2.2 can result in the tumor specificity observed. After intravenous injection, fluorescently labeled RNA complexed with polyethylenimine (PEI) was enriched in lungs but also in liver, spleen and kidney (data not shown). Thus, in our study, RNA delivery was not targeted to the tumor. Nevertheless, we observed tumor-specific apoptosis induction, which could be explained by cooperation between the following three mechanisms. First, melanoma cells express high levels of BCL2 to prevent spontaneous tumor cell apoptosis[15,17], whereas in normal cells all checkpoints of apoptosis are intact and inhibition of BCL2 alone is not sufficient for apoptosis induction. This is supported by our data comparing B16 tumor cells to mouse fibroblasts as well as human melanoma cells to primary human melanocytes. Second, in our hands, RIG-I activation is sufficient to induce apoptosis in B16 tumor cells and human melanoma cells but not in normal cells such as mouse fibroblasts, human fibroblasts and human melanocytes. Third, B16 melanoma cells are much more sensitive to killing by activated NK cells, strongly upregulate MHC class I expression and secrete high amounts of IP-10 only after transfection with 3p-siRNA. Therefore, we hypothesize that RIG-I–mediated activation of the type I IFN system in tumor

cells leads to changes on the cell surface that predispose these cells for NK cell attack and destruction, similar to what has been previously proposed[26].

Our studies show that treatment with 3p-siRNA can be extended to other models of tumorigenesis. We found that 3p-siRNA had antitumor activity against melanomas derived from primary cutaneous tumors in Hgf–*Cdk4*^{R24C} mice. The Hgf–*Cdk4*^{R24C} mouse melanoma model resembles the expected clinical situation in individuals with melanoma much more closely, first because melanomas arise as a consequence of genetic alterations similar to those observed in humans and second because melanomagenesis can be promoted by ultraviolet irradiation. Repeated administration of 3p-2.2 resulted in a significant delay in tumor growth in this model. We also observed antitumor efficacy of 3p-siRNA in a syngeneic colon carcinoma model in BALB/c mice. Furthermore, we provide evidence that the approach can be adapted to the human system. A *BCL2*-specific 3p-siRNA mediated both gene silencing and RIG-I activation in human melanoma cells leading to apoptosis, whereas melanocytes and fibroblasts were resistant to apoptosis induction. On the basis of these observations, we think that the principles of this approach show promise for clinical translation.

The gene silencing activity of such bifunctional 3p-siRNA molecules can be directed to any given molecularly defined genetic event that governs tumor cell survival. A combination of siRNA sequences selected for different tumor-related genes is feasible. New targets identified by functional screening in tumor cells can directly be imported into this bifunctional RNA system. This will advance the medical community's ability to attack the tumor from different biological angles, which we think is required to effectively counteract tumor cell survival, plasticity and immune escape. Despite the relative tumor specificity seen in our study, this strategy will be further improved by targeted delivery of the RNA to tumor tissue.

METHODS

RNA. We purchased chemically synthesized RNA oligonucleotides from Eurogentec or MWG-BIOTECH AG. A detailed list of all chemically synthesized RNA oligonucleotides is provided in **Supplementary Table 1**. In some experiments, we used single-stranded polyriboadenosine (PolyA) or nonsilencing siRNAs as controls (**Supplementary Table 1**). We synthesized *in vitro*–transcribed RNAs as previously described[11]. More details and a complete list of all *in vitro* transcription templates are provided in **Supplementary Table 2** and **Supplementary Methods** online.

Cell culture and transfection of RNA *in vitro*. The culture of mouse and human tumor cell lines and all primary cells is described in the **Supplementary Methods**. Approval from the Ethikkommission der Medizinischen Fakultät der Ludwig-Maximilians-Universität München and informed consent of the donors were obtained for all studies with human primary cells. We transfected melanoma cells, melanocytes and fibroblasts with RNAs (1 μg ml^{-1}) for 24 h with Lipofectamine 2000 or Lipofectamine RNAiMAX (both from Invitrogen) according to the manufacturer's protocol. We transfected dendritic cells as well as enriched lymphocyte subsets with 200 ng of nucleic acid with 0.5 μl of Lipofectamine in a volume of 200 μl.

Mice and injection of RNAs *in vivo*. We purchased female C57BL/6 and BALB/c mice from Harlan-Winkelmann. Mice were 6–12 weeks of age at the beginning of the experiments. Mouse studies were approved by the local regulatory agencies (Regierung von Oberbayern, and Regierung von Köln). *Ddx58*-, *Ifih1*-, *Tlr7*- and *Ifnar1*-deficient mice and CD11c-DTR mice were established as previously described[27–30]. For tumor treatment, we used *Tlr7*- or *Ifnar1*-deficient mice that were crossed into the C57BL/6 genetic background for at least ten generations. Hgf–*Cdk4*^{R24C} mice were bred as previously described[25]. We intravenously injected RNAs after complexation with *in vivo*–jetPEI (201-50, Biomol) according to the manufacturer's protocol. Briefly, for each mouse we mixed 10 μl of *in vivo*–jetPEI with 50 μg of nucleic acids (N:P ratio of 10:1, that is, 10 nitrogen residues of jetPEI per DNA phosphate) in a volume of 200 μl 5% glucose solution and incubated the mixture for 15 min. For systemic dendritic cell depletion, we injected CD11c-DTR transgenic mice intraperitoneally with 100 ng of diphteria toxin in PBS (Sigma D-0564). We confirmed CD11c^{+} depletion by flow cytometry and treated mice with jetPEI-complexed RNA 24 h after diptheria toxin injection.

Tumor treatment and lymphocyte depletion. We experimentally induced lung metastases by injection of 4×10^5 B16 melanoma cells into the tail vein. For tumor treatment, we administered 50 μg of RNA complexed with jetPEI in a volume of 200 μl on days 3, 6 and 9 after tumor challenge by retro-orbital or tail vein injection. Fourteen days after tumor challenge, we counted the number of macroscopically visible melanoma metastases on the surface of the lungs. We then snap-froze the tissue in liquid nitrogen. We depleted NK cells and CD8^{+} T cells as previously described[31]. Challenge and treatment of serially transplanted primary cutaneous melanomas derived from Hgf–*Cdk4*^{R24C} mice and of C26 colon carcinomas are described in the **Supplementary Methods**.

Verification of siRNA-mediated gene silencing. To confirm efficient gene silencing *in vitro* and *in vivo*, we performed western blot analyses with lysed tumor cells and tumor tissue, flow cytometric analyses with single-cell suspensions, and quantitative RT-PCR and 5′-RACE analyses with extracted total RNA (**Supplementary Methods**). For rescue experiments, we transfected B16 melanoma cells stably with a mutated *Bcl2* cDNA specifically designed to disrupt the target cleavage site of the *Bcl2*-specific siRNA 2.2 without affecting the amino acid sequence of the Bcl-2 protein (**Supplementary Fig. 9** and **Supplementary Methods**).

Analyses of cytokine production and immune activation. We measured the production of cytokines in culture supernatants by ELISA, assessed the activation of dendritic cells and NK cells by flow cytometry and determined the stimulation of NK cell lytic activity against tumor cells with a standard ^{51}Cr release assay (**Supplementary Methods**). To determine the activation of type I IFN in tumor cells, we used a luciferase-based IFN-β reporter gene assay as described in the **Supplementary Methods**.

Measurement of apoptotic cell death. We measured the induction of apoptosis in cells cultured *in vitro* or freshly isolated *ex vivo* by staining for annexin V on the cell surface and by using flow cytometry. Alternatively, we quantified viable cells with a fluorimetric assay (CellTiter-Blue Cell Viability Assay, Promega) *in vitro*. We further verified apoptosis *in vivo* by immunohistochemistry with TUNEL staining (**Supplementary Methods**).

Statistical analyses. We determined the statistical significance of differences by the two-tailed Student's *t*-test. For the analysis of the tumor experiments, we used the nonparametric Mann-Whitney *U* test to compare the mean values between two groups. We performed statistical analysis with SPSS software. *P* values < 0.05 were considered significant.

Note: Supplementary information is available on the Nature Medicine website.

ACKNOWLEDGMENTS

This study was supported by grant Biofuture 0311896 of the Bundesministerium für Bildung und Forschung and by grants SFB 704, SFB 670, KFO115 and KFO177 of the Deutsche Forschungsgemeinschaft to G. Hartmann; by grants Tu90-6/1 of the Deutsche Forschungsgemeinschaft and 10741 of the Deutsche Krebshilfe to T.T.; by grant 107805 of the Deutsche Krebshilfe to R.B.; by Graduiertenkolleg 1202 to C.M., M.B. and T.S.; by LMUexcellent (CIPSM 114, research professorship), and by SFB-TR 36 and En 169/7-2 of the Deutsche Forschungsgemeinschaft to S.E. and C. Bourquin. This work is part of the theses of C.M. and M.B. at the University of Munich and of M.R. and J.L. at the University of Bonn. We thank A. Dann for excellent technical assistance, T. Maniatis (Harvard University) and J. Chen (University of Texas Southwestern Medical Center) for providing IFN-β–Luc reporter plasmids and wild-type pPME-myc NS3-4A (NS3-4A), respectively, T. Fujita (Institute for Virus Research, Kyoto University) for providing Rig-I and the empty control vector and

C. Borner (Institute of Molecular Medicine and Cell Research, University of Freiburg) for providing wild-type mouse Bcl-2 (mBcl-2/pcDNA).

AUTHOR CONTRIBUTIONS

H.P., R.B., T.T. and G. Hartmann designed the research; H.P., C.M., R.B., D.T., S.S.M., M.R., S.K., E.G., J.L., J.H., A.S., M.B., T.S., D.A., M.N., M.P., C. Berking and T.T. performed experiments; H.P., R.B., S.E., C. Bourquin, G. Häcker, C. Berking, R.M., V.H., S.R., T.T. and G. Hartmann conducted the data analyses; E.K., U.K., D.B., J.R., H.K. and S.A. provided genetically deficient mice and key research tools; H.P., C.M., R.B. and T.T. prepared the figures; and H.P., T.T. and G. Hartmann wrote the manuscript.

COMPETING INTERESTS STATEMENT

The authors declare competing financial interests: details accompany the full-text HTML version of the paper at http://www.nature.com/naturemedicine/.

Published online at http://www.nature.com/naturemedicine/
Reprints and permissions information is available online at http://npg.nature.com/reprintsandpermissions/

1. Hanahan, D. & Weinberg, R.A. The hallmarks of cancer. *Cell* **100**, 57–70 (2000).
2. Bui, J.D. & Schreiber, R.D. Cancer immunosurveillance, immunoediting and inflammation: independent or interdependent processes? *Curr. Opin. Immunol.* **19**, 203–208 (2007).
3. Rubin, B.P., Heinrich, M.C. & Corless, C.L. Gastrointestinal stromal tumour. *Lancet* **369**, 1731–1741 (2007).
4. Curiel, T.J. Tregs and rethinking cancer immunotherapy. *J. Clin. Invest.* **117**, 1167–1174 (2007).
5. Uno, T. *et al.* Eradication of established tumors in mice by a combination antibody-based therapy. *Nat. Med.* **12**, 693–698 (2006).
6. Obeid, M. *et al.* Calreticulin exposure dictates the immunogenicity of cancer cell death. *Nat. Med.* **13**, 54–61 (2007).
7. Schlee, M., Hornung, V. & Hartmann, G. siRNA and isRNA: two edges of one sword. *Mol. Ther.* **14**, 463–470 (2006).
8. Pei, Y. & Tuschl, T. On the art of identifying effective and specific siRNAs. *Nat. Methods* **3**, 670–676 (2006).
9. de Fougerolles, A., Vornlocher, H.P., Maraganore, J. & Lieberman, J. Interfering with disease: a progress report on siRNA-based therapeutics. *Nat. Rev. Drug Discov.* **6**, 443–453 (2007).
10. Yoneyama, M. *et al.* The RNA helicase RIG-I has an essential function in double-stranded RNA–induced innate antiviral responses. *Nat. Immunol.* **5**, 730–737 (2004).
11. Hornung, V. *et al.* 5′-triphosphate RNA is the ligand for RIG-I. *Science* **314**, 994–997 (2006).
12. Pichlmair, A. *et al.* RIG-I–mediated antiviral responses to single-stranded RNA bearing 5′-phosphates. *Science* **314**, 997–1001 (2006).
13. Yoneyama, M. & Fujita, T. Function of RIG-I–like receptors in antiviral innate immunity. *J. Biol. Chem.* **282**, 15315–15318 (2007).
14. Kim, D.H. *et al.* Interferon induction by siRNAs and ssRNAs synthesized by phage polymerase. *Nat. Biotechnol.* **22**, 321–325 (2004).
15. Miller, A.J. & Mihm, M.C. Jr. Melanoma. *N. Engl. J. Med.* **355**, 51–65 (2006).
16. Danial, N.N. & Korsmeyer, S.J. Cell death: critical control points. *Cell* **116**, 205–219 (2004).
17. McGill, G.G. *et al.* Bcl2 regulation by the melanocyte master regulator Mitf modulates lineage survival and melanoma cell viability. *Cell* **109**, 707–718 (2002).
18. Hornung, V. *et al.* Sequence-specific potent induction of IFN-α by short interfering RNA in plasmacytoid dendritic cells through TLR7. *Nat. Med.* **11**, 263–270 (2005).
19. Judge, A.D. *et al.* Sequence-dependent stimulation of the mammalian innate immune response by synthetic siRNA. *Nat. Biotechnol.* **23**, 457–462 (2005).
20. Kawai, T. & Akira, S. Innate immune recognition of viral infection. *Nat. Immunol.* **7**, 131–137 (2006).
21. Kato, H. *et al.* Cell type-specific involvement of RIG-I in antiviral response. *Immunity* **23**, 19–28 (2005).
22. Melchjorsen, J. *et al.* Activation of innate defense against a paramyxovirus is mediated by RIG-I and TLR7 and TLR8 in a cell-type-specific manner. *J. Virol.* **79**, 12944–12951 (2005).
23. Kawai, T. *et al.* IPS-1, an adaptor triggering RIG-I– and Mda5-mediated type I interferon induction. *Nat. Immunol.* **6**, 981–988 (2005).
24. Meylan, E. *et al.* Cardif is an adaptor protein in the RIG-I antiviral pathway and is targeted by hepatitis C virus. *Nature* **437**, 1167–1172 (2005).
25. Tormo, D. *et al.* Therapeutic efficacy of antigen-specific vaccination and Toll-like receptor stimulation against established transplanted and autochthonous melanoma in mice. *Cancer Res.* **66**, 5427–5435 (2006).
26. Stetson, D.B. & Medzhitov, R. Antiviral defense: interferons and beyond. *J. Exp. Med.* **203**, 1837–1841 (2006).
27. Diebold, S.S., Kaisho, T., Hemmi, H., Akira, S. & Reis e Sousa, C. Innate antiviral responses by means of TLR7-mediated recognition of single-stranded RNA. *Science* **303**, 1529–1531 (2004).
28. Kato, H. *et al.* Differential roles of MDA5 and RIG-I helicases in the recognition of RNA viruses. *Nature* **441**, 101–105 (2006).
29. Muller, U. *et al.* Functional role of type I and type II interferons in antiviral defense. *Science* **264**, 1918–1921 (1994).
30. Kamphuis, E., Junt, T., Waibler, Z., Forster, R. & Kalinke, U. Type I interferons directly regulate lymphocyte recirculation and cause transient blood lymphopenia. *Blood* **108**, 3253–3261 (2006).
31. Mocikat, R. *et al.* Natural killer cells activated by MHC class I^{low} targets prime dendritic cells to induce protective CD8 T cell responses. *Immunity* **19**, 561–569 (2003).